Journal of Hazardous Materials 196 (2011) 402–411

Contents lists available at SciVerse ScienceDirect

Journal of Hazardous Materials

journal homepage: www.elsevier.com/locate/jhazmat

Reconstruction of metal pollution and recent sedimentation processes in Havana Bay (Cuba): A tool for coastal ecosystem management

M. Díaz-Asencio[a,*], J.A. Corcho Alvarado[b], C. Alonso-Hernández[a], A. Quejido-Cabezas[c], A.C. Ruiz-Fernández[d], M. Sanchez-Sanchez[c], M.B. Gómez-Mancebo[c], P. Froidevaux[b], J.A. Sanchez-Cabeza[e]

[a] Centro de Estudios Ambientales de Cienfuegos, Carretera Castillo de Jagua, Cienfuegos, CITMA-Cienfuegos, Cuba
[b] Institute of Radiation Physics (IRA), University Hospital and University of Lausanne, Rue du Grand-Pré 1, 1007 Lausanne, Switzerland
[c] Centro de Investigaciones Energéticas, Medioambientales y Tecnológicas (CIEMAT), Madrid, Spain
[d] Universidad Nacional Autónoma de México. ICMyL, Mazatlán, Mexico
[e] Institute of Environmental Science and Technology, and Physics Department, Universitat Autónoma de Barcelona, 08193 Bellaterra, Barcelona, Spain

ARTICLE INFO

Article history:
Received 20 June 2011
Received in revised form
12 September 2011
Accepted 12 September 2011
Available online 16 September 2011

Keywords:
Pollutants
^{210}Pb
^{239,240}Pu
^{137}Cs
Sediment dating
Havana Bay

ABSTRACT

Since 1998 the highly polluted Havana Bay ecosystem has been the subject of a mitigation program. In order to determine whether pollution-reduction strategies were effective, we have evaluated the historical trends of pollution recorded in sediments of the Bay. A sediment core was dated radiometrically using natural and artificial fallout radionuclides. An irregularity in the ^{210}Pb record was caused by an episode of accelerated sedimentation. This episode was dated to occur in 1982, a year coincident with the heaviest rains reported in Havana over the XX century. Peaks of mass accumulation rates (MAR) were associated with hurricanes and intensive rains. In the past 60 years, these maxima are related to strong El Niño periods, which are known to increase rainfall in the north Caribbean region. We observed a steady increase of pollution (mainly Pb, Zn, Sn, and Hg) since the beginning of the century to the mid 90s, with enrichment factors as high as 6. MAR and pollution decreased rapidly after the mid 90s, although some trace metal levels remain high. This reduction was due to the integrated coastal zone management program introduced in the late 90s, which dismissed catchment erosion and pollution.

1. Introduction

Havana Bay is one of the largest and most important estuaries in the Cuban Island. The economic, commercial and recreational values of the bay have been, however, threatened by pollution and the reduction of water depth due to infilling [1]. The environmental degradation of the bay ecosystem has been intensified in the past decades due to the fast economical growth of Havana City. This one has become the most contaminated bay in the island [2]. In order to rehabilitate this marine ecosystem, several pollution-reduction measures have been implemented over the past decade.

Reliable information about the input of pollutants to Havana Bay is however required for evaluating the impact of the environmental management practices. In the absence of long-term monitoring data, sedimentary records can provide retrospective information about the past inputs of pollutants into aquatic environments. Pollutants such as heavy metals often have a strong affinity for particle surfaces and, therefore, accumulate in the sediments. Hence, dated sediment profiles of major and trace elements can be used to obtain reliable information about the extent and history of pollution and sedimentary conditions [3–7].

The quantitative reconstruction of a contaminant input into an aquatic system requires a good sediment chronology. The most widely used method for dating recent marine and lacustrine sediments is based on the examination of ^{210}Pb profiles. The natural radionuclide ^{210}Pb ($T_{1/2}$ = 22.23 yr) enters the aquatic environment mainly by atmospheric deposition; however it can be produced in situ, in the water column and the sediments, by decay of its precursor radionuclide ^{226}Ra ($T_{1/2}$ = 1600 yr). The ^{210}Pb dating methods are based on the radioactive disequilibrium between the ^{210}Pb and ^{226}Ra [8,9]. ^{210}Pb has shown to be an ideal tracer for dating aquatic sediments deposited during the last 100–150 years, a period of time with significant environmental changes due to industrialization and population growth.

^{210}Pb dating should be always corroborated by an additional chronostratigraphic marker in the same sediment core [10,11]. Among the most commonly used time markers we find anthropogenic fallout radionuclides such as ^{137}Cs, ^{239,240}Pu or ^{241}Am

* Corresponding author.
E-mail address: misael@ceac.cu (M. Díaz-Asencio).

0304-3894/$ – see front matter © 2011 Elsevier B.V. All rights reserved.
doi:10.1016/j.jhazmat.2011.09.037

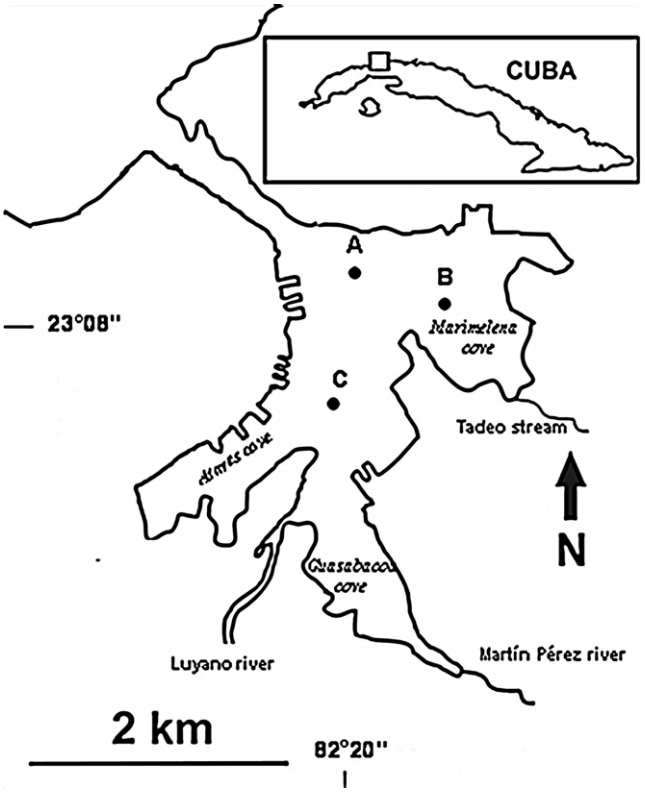

Fig. 1. Map of Havana Bay, with sampling station.

[13]. The onset of anthropogenic radionuclides, originating from the atmospheric nuclear weapon tests (early 1950s) and their peak value in 1963 [12] have been widely used as time markers in numerous marine and lacustrine studies [13–15].

In this work we reconstructed the historical trends of pollutants entering the Havana Bay by analyzing their sediment concentration profiles. The chronology of the sediment core was based on the ^{210}Pb dating method. Due to the low levels of ^{137}Cs found in the sediments, the chronology was further validated with ^{239,240}Pu and ^{241}Am fallout radionuclides. Enrichment factors and fluxes of pollutants were used to describe the history of pollutions in this aquatic ecosystem. A full geochemical analysis was undertaken to look at possible impacts of changing catchment sources, diagenesis, and atmospheric contamination. The potential origin of the most important pollutants and the impact of the pollution-reduction measures taken to protect the Havana Bay ecosystem are also discussed. Despite the large number of studies of pollution in coastal environments, only a few have been conducted in the Caribbean region. Hence, this study provides important information about pollution trends in a coastal ecosystem of this tropical region.

2. Site description

Havana Bay (NW Cuba) is located aside Havana City, is a typical enclosed bay with a catchment area of about 68 km^2. It is characterized by a mean depth of 10 m, an area of 5.2 km^2 and a water mean residence time of 7–9 days [1]. The bay is an estuary with deltaic systems in the fluvial discharge zones of the Luyano and Martin Perez rivers, and the Tadeo, Matadero, Agua Dulce and San Nicolas streams (Fig. 1).

The population density, commercial and harbors activities in Havana City increased significantly since 1850. The city became a key transshipment point between Europe and America in the 19th century. Nowadays, the port of Havana receives about 50% of the ships arriving to the country. Agriculture and intensive forest exploitation in the bay catchment increased soil erosion and, therefore, sediment input to the Bay. Industrial activities began in the 1850s with the construction of oil refineries, electric power plants and gas production [2,16]. The area of Havana experienced a fast economical growth during the 20th century, with a high diversity of industries and commercial activities, and a large population growth that required massive urbanization (from 250,000 inhabitants in 1899 to 2.2 million inhabitants in 2001).

The anarchic growth of many activities over the past 400 years has caused severe damages to the natural resources and facilities of the Havana Bay. The damages have been intensified by the lack of waste treatment facilities [2,17,18]. The bay receives contaminants from numerous sources such as an oil refinery, power stations, urban and industrial wastewaters, three shipyards, riverine and stream discharges, and atmospheric fallout [1].

3. Sampling and laboratory methods

3.1. Sampling

In February 2008, sediment cores were collected with an UWITEC corer avoiding dredged areas of the bay (Fig. 1). In order to optimize analytical time and resources, we chose the cores with the best likelihood to show good temporal record (section 1 of Supporting information). We sampled three sediment cores from the station B (23°08.107′N 82°20.043′) at a water depth of 8 m (Fig. 1): one core for radionuclides, metals and grain size analysis; one for organic pollutants (not reported here) and one was kept frozen for future analysis. The sediment core was vertically extruded and sliced into 1 cm sections. Each section was dried at 45 °C, sieved through a 1 cm sieve and homogenized. The mud content in the sediments showed a slight decreasing trend from 15 cm depth to the surface. The sediments also showed a strong change in color at about 15 cm depth.

3.2. Laboratory analyses

Grain size was determined by standard methods of sieving and pipetting analysis [19]. Content of organic matter for each section was estimated by the loss on ignition method (LOI: 450 °C, for 8 h). The content of total carbon and nitrogen was measured by using a CHN analyzer (LECO TRUSPEC). Total carbon was measured as CO_2 with an infrared detector. N_2 was measured by using a thermal conductivity detector. Inorganic carbon was quantified by using an infrared detector (SSM-500, Shimadzu) after sample acidification with phosphoric acid and heating (200° C). Major and trace elements were measured by Wavelength Dispersion X-Ray Fluorescence Spectrometry (WDXRF) using a Panalytical system (AXIOS) with Rhodium tube. Total mercury concentrations were determined by using an Advanced Mercury Analyser (LECO AMA-254, detection limit of 0.01 ng Hg).

3.3. Sediment dating

The chronology of the sediment cores was determined by the ^{210}Pb method (section 2.3 of Supporting information). Sediment samples were placed in sealed plastic containers and stored for at least three weeks in order to allow ^{226}Ra to reach equilibrium with its daughter nuclides. ^{226}Ra was then analysed by high-resolution gamma spectrometry, using a low-background intrinsic Ge coaxial detector ORTEC model GX10022. ^{226}Ra was determined via the 352 keV emitted by its daughter nuclide ^{214}Pb in equilibrium. Supported $^{210}Pb_{sup}$ was derived from the assumption of equilibrium with ^{226}Ra. The total ^{210}Pb activity was determined by high-resolution α spectrometry of its decay product ^{210}Po, assumed

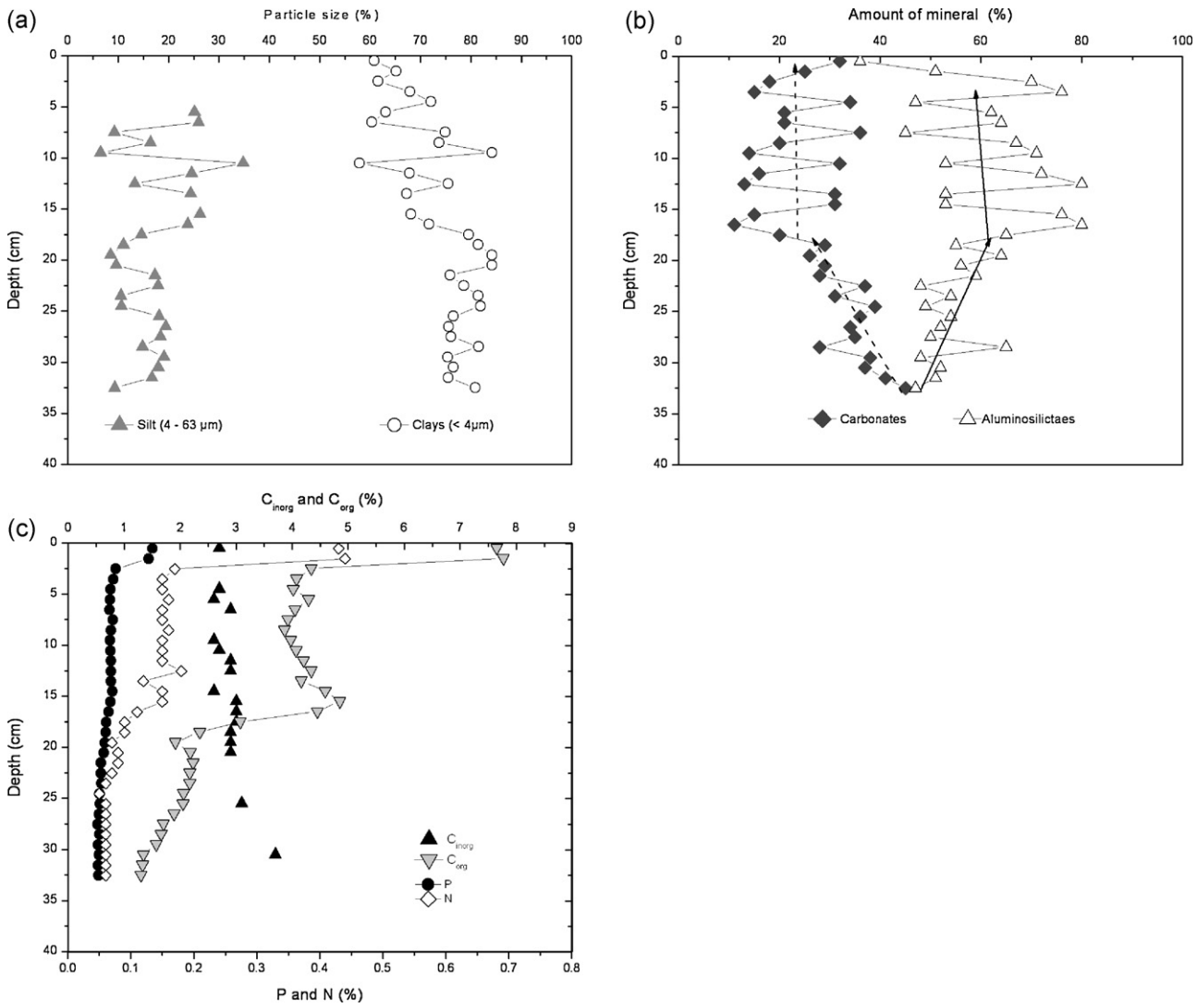

Fig. 2. Profiles in core B of (a) particle size distribution, (b) carbonates and aluminisilicates distribution, and (c) organic (C_{org}) and inorganic (C_{inorg}) carbon, phosphorous (P) and nitrogen (N).

to be at equilibrium. Aliquots (0.5 g) of dry sediment were spiked with ^{209}Po as a yield tracer and dissolved by adding a mixture of 1:1:0.5 HNO_3 + HCl + HF using an analytical microwave system [20]. ^{210}Po was electrodeposited onto silver discs [21,22] and counting was done in an integrated Camberra alpha spectrometer with ion implanted planar silicon detectors (active area of 450 mm^2; and 18 keV of nominal resolution). The ^{210}Pb in excess ($^{210}Pb_{ex}$) to the ^{210}Pb supported by ^{226}Ra ($^{210}Pb_{sup}$) was determined by subtracting the $^{210}Pb_{sup}$ from the total activity of ^{210}Pb measured in each layer. $^{210}Pb_{ex}$ was then introduced in the models in order to obtain the sedimentation rate (section 2.3 of Supporting information).

Measurements of ^{137}Cs, ^{239,240}Pu and ^{241}Am were used to validate the ^{210}Pb dating models. ^{137}Cs was measured via its emission at 662 keV by high-resolution gamma spectrometry. The sediment samples were then crushed and ashed at 550 °C for 48 h prior to the radiochemical analyses of ^{239,240}Pu and ^{241}Am. Composite samples were prepared by mixing layers. The method combines high-pressure microwave digestion for the dissolution of the sample and the highly selective extraction chromatographic resins TEVA and DGA (Triskem International, France) for the separation and purification of Pu and Am [23]. The alpha sources were prepared by electrodeposition onto stainless steel discs [24]. High-resolution α-spectrometry was performed on a α-spectrometer with PIPS detectors (Alpha Analyst, Canberra Electronic).

4. Results

4.1. Characteristic of the sediments

The sediments are predominantly fine and displayed small variations in grain size in the overall samples (Fig. 2a). The sediments consisted mainly of clay (<4 μm, 58–85%), and silt and very fine sand (>4 μm, 15–42%) sized particles. In the upper 5 cm, the percent of silt and very fine to coarse sand sized particles increased slightly (Fig. 2a).

The sediments were mainly composed of carbonates (11–45%) and aluminosilicates (40–80%). The mineral composition of the sediments did not change significantly from the bottom of the core up to 20 cm depth (Fig. 2b). However, from 20 cm depth up to the surface large variations were observed with the amount of carbonates correlating negatively to the amount of alumino-silicates (Fig. 2b).

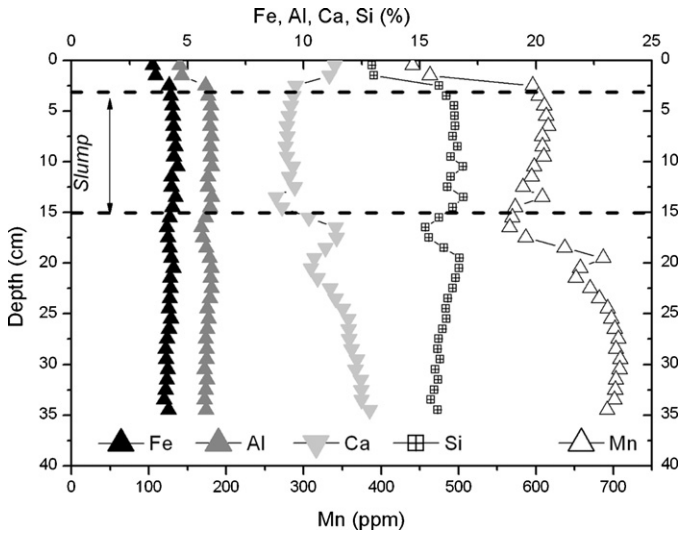

Fig. 3. Profiles of Si, Ca, Fe, Al and Mn in core B. Uncertainties were below 2% for all elements. The dashed line indicates the slump.

The amount of carbonates showed a general trend to decrease towards the surface, but it increased rapidly in the top 4 cm (Fig. 2b).

The content of inorganic carbon (C_{inorg}) in the sediments was almost constant along the whole core; but the organic carbon (C_{org}) showed a surface maximum and then decreased with depth depicting two zones of rapid change (at 2–3 cm, and at 16–17 cm depth; Fig. 2c). The large percentage of C_{org} in the top 2–3 cm may be related to a change in the sources of organic matter, more complex and less biodegradable, typical of industrial organic wastes. However, the increase of organic matter may be also related to the reduction of particles observed in the Bay over the past decades. In the segment 3–16 cm, C_{org} was nearly constant around 4%; then, below 16 cm depth, C_{org} decayed to about 1.5% (Fig. 2c). Similarly to the pattern of C_{org}, nitrogen (N) and phosphorous (P) profiles showed increasing trends towards the surface, with nearly constant concentrations between 3 and 16 cm depth (Fig. 2c).

4.2. Major and tracer elements in the sediment core

The concentration profiles of Al, Fe, Si, and Mn showed a slight decrease in the two uppermost layers, but no significant changes below 3 cm depth (Fig. 3). The Ca content showed an opposite trend to Al (Fe, Si), with slightly higher concentrations at the surface (Fig. 3). In fact, Ca, which is probably in the form of biogenic carbonates, acts as a dilute of the trace metal concentrations in the bulk sediments. A slight change in the profiles is observed at 15–20 cm, which probably indicates the input of sediments with high content of Ca (Fig. 3).

The concentration profiles of Pb, Zn, S, Hg, Sn and Cr in the sediment core showed similar increasing trends towards surface (Fig. 4). Maximum concentrations for Zn (450 mg kg^{-1}), Pb (123 mg kg^{-1}) and S (1.4 mg kg^{-1}) were observed at the core surface, while for Hg (1.4 mg kg^{-1}), Sn (18.6 mg kg^{-1}) and Cr (365 mg kg^{-1}) the maximum concentrations were found at depths between 5 and 15 cm. The maximum concentrations are comparable to the concentrations found in other polluted coastal sediments such as Porto Marghera in Italy [25], Halifax Harbor in Nova Scotia [26] and Barcelona in Spain [27]. The similarities in the Pb, Zn and Sn profiles (linear correlation $R^2 > 0.9$ and $p < 0.01$ for each combination) suggest that these elements possibly originated from the same source and/or that the geochemical affinities to the sediment particles are similar. Pb, Zn, Hg, Sn, Cr and S profiles showed a plateau between 3 and 15 cm depth suggesting a similar time of deposition for the whole segment (e.g. an episodic event).

4.3. Radionuclide profiles and sediment chronology

The $^{210}Pb_{ex}$ profile has non-monotonic features suggesting irregularities in the process of sediment accumulation (Fig. 5a). The surface $^{210}Pb_{ex}$ activities were around to 230 Bq kg^{-1} (Fig. 5a), relatively high compared to activities found in other studies from Havana Bay [28] and from other Cuban coastal locations [4,29]. A detailed analysis of the $^{210}Pb_{ex}$ distribution with depth suggests that the record can be divided into three distinct segments. At the top (0–3 cm) and bottom (15–35 cm) sections of the sediment core, $^{210}Pb_{ex}$ declined exponentially with depth, indicating regular sedimentation. However, $^{210}Pb_{ex}$ was almost constant throughout the 3–15 cm segment of the core. A flattening of $^{210}Pb_{ex}$ indicates either a dilution of the ^{210}Pb atmospheric flux by sediment mixing, accelerating sedimentation and/or the occurrence of slumps due to, for example, heavy rains (typical in this tropical region).

The trends observed in the profiles of $^{210}Pb_{ex}$ (Fig. 5a), C_{org}, P, N (Fig. 2c) and some major and trace elements (Figs. 3 and 4) suggest that most probably the section from 3 to 15 cm was instantly deposited as a result of an episodic event or slump. This is also supported by the color change of the sediment core at about 15 cm

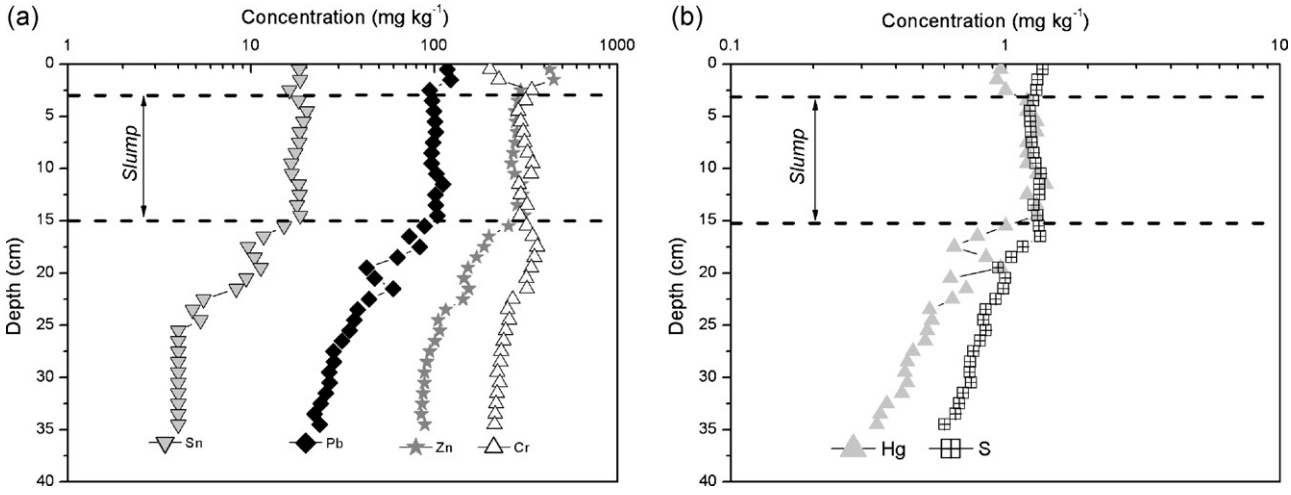

Fig. 4. Profiles of (a) Pb, Zn, Sn and Cr; and b) S and Hg in core B. The uncertainties were: Pb (<1%); Zn (<1%); S (<2%), Hg (<0.5%), Sn (<4%), Cr (<1%). The dashed line indicates the slump.

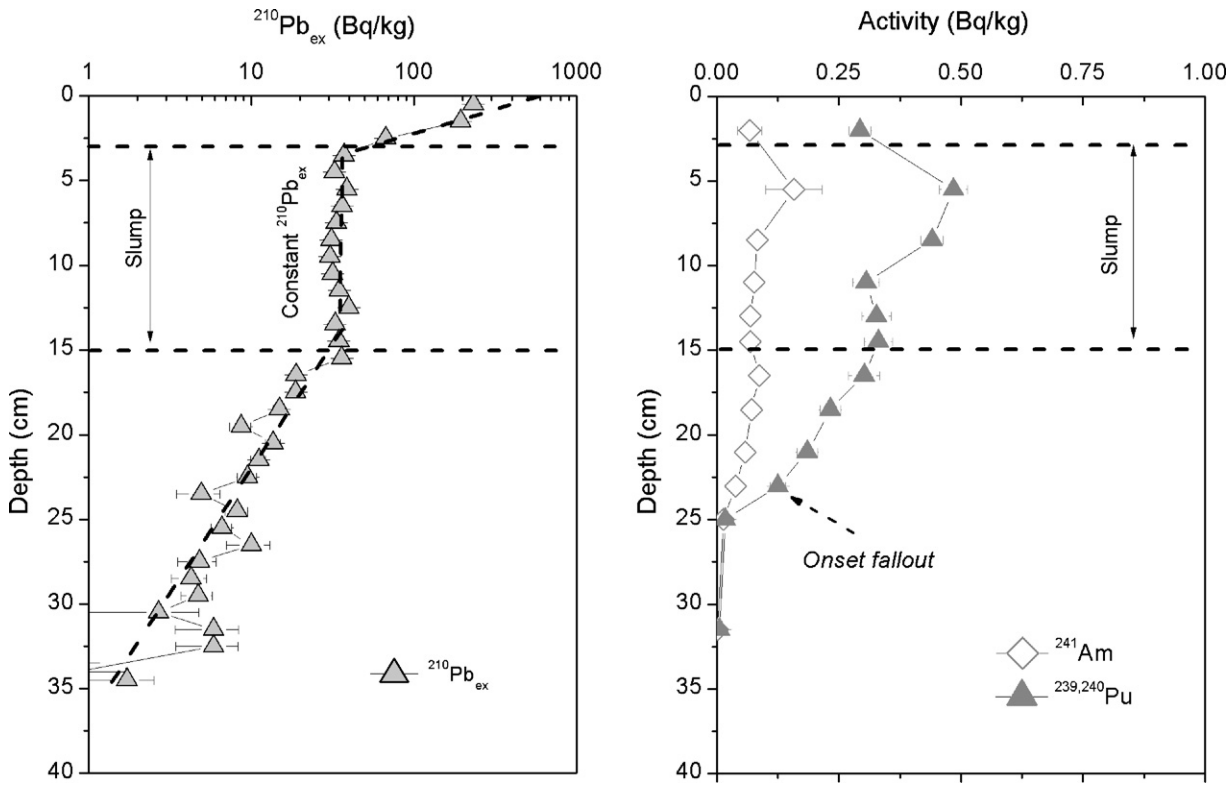

Fig. 5. Profiles of the activities of (a) $^{210}Pb_{ex}$, (b) ^{241}Am and $^{239,240}Pu$ in core B. The dashed line indicates the slump.

depth (Table 1 of Supporting information). Sediment packages (slumps) are commonly observed in coastal areas, especially where riverine inputs are important. We conclude that about 87.3 kg m^{-2} were rapidly deposited (slump) in this zone of the Havana Bay.

While the ^{137}Cs signal in the sediments was very low (<1.8 Bq kg^{-1}), close to the detection limit; $^{239,240}Pu$ and ^{241}Am were detected in the sediment core at levels up to 0.50 Bq kg^{-1} and 0.16 Bq kg^{-1}, respectively (Fig. 5b). The first appearance of Pu and Am radionuclides in the sediment core (fallout onset) is found at 23 cm, which is a composite of the 22–23 and 23–24 cm layers (Fig. 5b). Despite the low ^{137}Cs activities in the sediments, its first appearance was also found at about 22 cm. These results indicate that the first appearance of the anthropogenic fallout radionuclides (1952) is indeed associated with the 22–24 cm depth horizon.

The vertical distributions of $^{239,240}Pu$ and ^{241}Am did not show a well developed peak corresponding to the expected radionuclide fallout maximum in 1963 (Fig. 5b). However, both profiles depicted slightly higher activities in the middle segment (3–15 cm) associated to an episodic deposition event. This episodic event was responsible for a large input of radionuclides from the catchment area. The significant input of radionuclides from the catchment, compared to the direct atmospheric input, is confirmed by the large $^{239,240}Pu$ inventory of in the core (60 Bq m^{-2}) compared to the expected Pu fallout inventory in Havana City (15–30 Bq m^{-2}; section 2.2 of Supporting information). The $^{239,240}Pu$ inventory in the core is 2–4 times higher than the expected Pu fallout inventory in Havana City and in other nearby regions in USA [30–33]. $^{239,240}Pu$ inventories higher than the expected fallout inventory have been commonly found in marine sediments from near shore or coastal zones, which are characterized by high particle fluxes [33,34]. Our results show that the site received a substantial sediment-associated radionuclide input from its catchment area in addition to the direct atmospheric input.

We used the Constant Flux (CF) model [8,9] after removing the segment 3–15 cm (slump), and obtained an average mass accumulation rate (MAR) of 1.6 kg m^{-2} y^{-1} and a ^{210}Pb flux of 137 Bq m^{-2} y^{-1}. These parameters are similar to those reported for other coastal regions of Cuba [4,29]. The CF MAR ranged from 0.4 to 3.8 kg m^{-2} y^{-1} (Fig. 6a and b), with a significant decrease in the past two decades. The CF ages agree well with the onset fallout determined from Pu and Am radionuclides (Fig. 6c). The sediment chronology was also constructed by the Constant Flux Constant Sedimentation (CFCS) model [35] in the same conditions as the CF model (section 2.3. of Supporting information). The results of both CFCS dating model in core B agree relatively well with the CF model (Fig. 6c). Therefore, the ages and MAR of the CF model, after removing the slump event, were used for the reconstruction of the pollution history of Habana Bay.

5. Discussion

5.1. Origin of major changes in sediment accumulation

As shown in Fig. 6b, the MAR peaks most likely correspond to the major hurricanes and intensives rains that affected the Havana area between 1910 and 1982 [36–38]. The slump was dated in 1982, a severe El Niño period in Cuba (1982–1983; [36,39]). The rainfall in 1982 was reported as the strongest in Havana over 60 years [36]. As a result of the heavy rains in 1982, coastal flooding affected the coastal areas of Havana with intensities not witnessed in the region since the Great Hurricane of 1926 [39]. A closer look to the MAR record shows that three of the recent peaks could be associated with years (1957 or 1965, 1972 and 1982) with a strong El Niño influence (Fig. 6b). Indeed, some studies have shown that during El Niño years there is a significant increase in the number of days with heavy precipitations in Cuba [39–42], and therefore an increase in the sedimentation rate due to watershed erosion. Studies in nearby regions have found similar patterns associated to the ENSO warm phases. For example, Jamaica (SE of Cuba) is more likely to

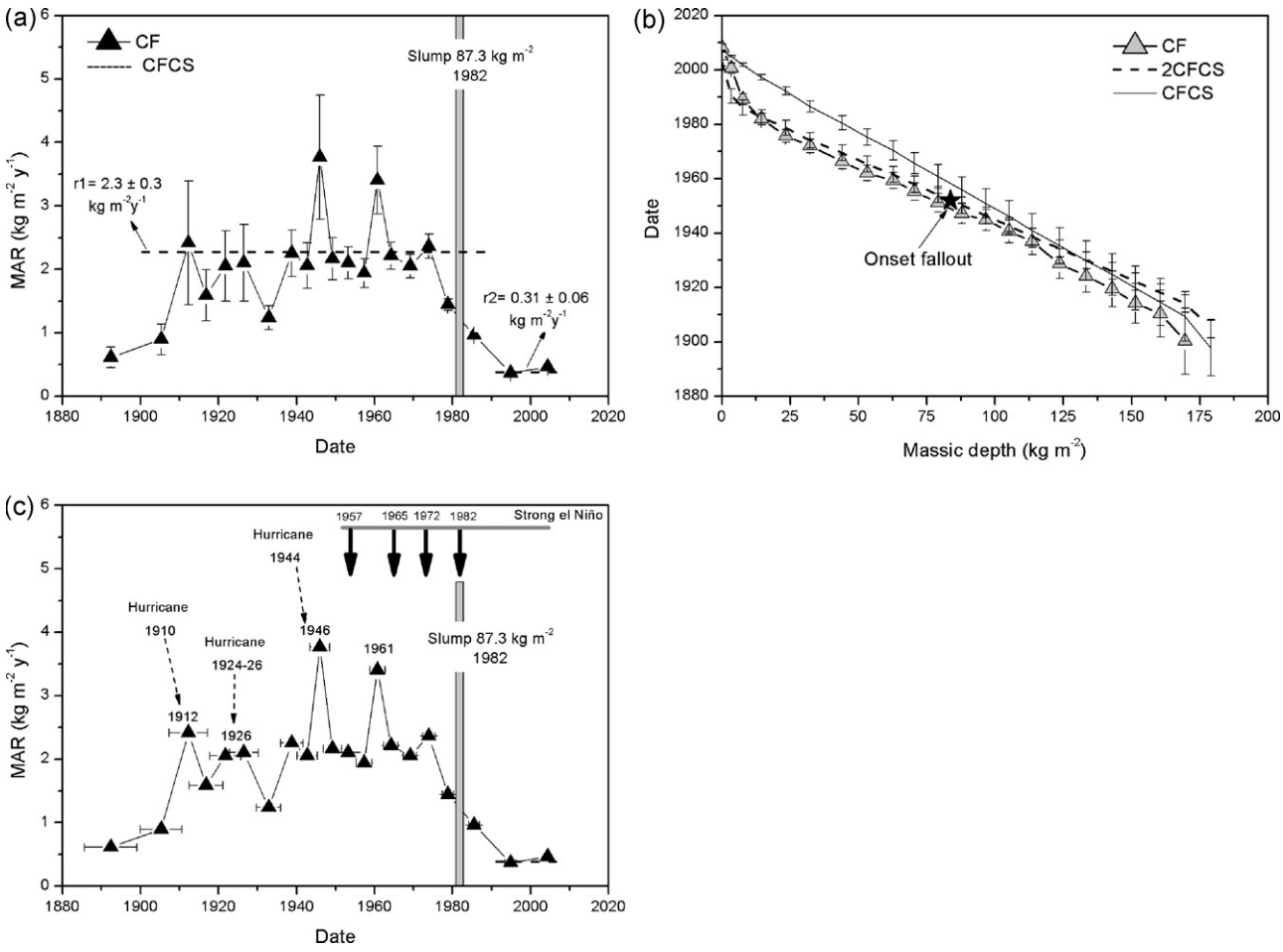

Fig. 6. Results of the application of the CF and CFCS dating models. (a and b) Temporal evolution of the CF MAR and the CFCS MAR. The date of occurrence of important climatic events such as cyclones, hurricanes and the years of strong El Niño events are also shown. (c) ^{210}Pb ages obtained with the CFCS and the CF models versus the massic depth (kg m^{-2}), without considering the slump from 3 to 15 cm depth. The location of the onset fallout is also indicated.

experience floods during May–July of years with warm phases [43]. In the region between Florida and the north Caribbean, an excess of rainfall also occurs during the early dry season for ENSO warm phases [44]. This rainfall excess during ENSO warm phases has been associated, for example, with a greater frequency of extra-tropical cyclone passages across the southern continental USA.

In the nineties, an ambitious coastal zone management program was implemented to restore the Havana Bay by acting on watershed erosion and pollution sources [16]. As a result, a significant reduction of solid suspended matter was observed in the Bay [45]. The low MARs observed in the upper section of core B (Fig. 6a) is similar to the ones observed at the end of the XIX century for other cores taken within the frame of this study (Table 4 of Supporting information). We concluded that the significant reduction of MAR over the past two decades is due to a combination of the effectiveness of the coastal zone management program implemented since 1998 and the economical contraction of Cuba in the early 90s due to the economic collapse of the socialist block.

5.2. Pollution history in the last 100 years

Identifying anthropogenic from natural sources of pollutants is essential to understand the pollution history recorded in the sediments. For this purpose, the comparison of the element content in the sediments with the pre-industrial background concentration is often used. The enrichment factor (EF) and pollutant fluxes were calculated in order to evaluate the pollution record of the Havana Bay ecosystem (section 2.1. of Supporting information).

Enrichments of Pb, Zn, Sn, S, Cr and Hg are already observed since 1900 (Fig. 7a and b), indicating that anthropogenic pollution sources were active during the whole XX century. Indeed, pollution was likely associated to old pre-industrial activities in the bay, such as forges and metal manipulation in shipyards (which provided services to a large fleet), leather manufacture, and sugar and derivatives production. The use of some natural heavy hydrocarbons such as tar (with high levels of S, Pb and Hg) to waterproof ships is reported to occur before 1700 [1].

The EFs increased significantly after 1950s, which corresponds to the period of economical development in Cuba and of fast population growth in Havana City. In the past two decades, the EFs of Pb, Zn and Sn were higher than 5 (500% increase) than the core bottom levels (Fig. 7a). These high EFs are likely a result of an increase of the pollutant specific concentrations due to the significant reduction of solid matter in Habana Bay over the past two decades [45].

For Sn and Hg, despite the significant increase of their EFs, the absolute fluxes have been decreasing since the 80s. This behavior can also be explained by the reduction of solid matter in the Bay over the past two decades as changes in their fluxes (Fig. 8) seem to be slightly modulated by changes in the MAR (Fig. 6a).

The anthropogenic fluxes of Pb, Zn, Sn, S, Hg and Cr into the sediments increased rapidly from the beginning of the century until the 1980s (Fig. 8), indicating an increasing impact from the urban and industrial activities around Havana Bay. However, these fluxes

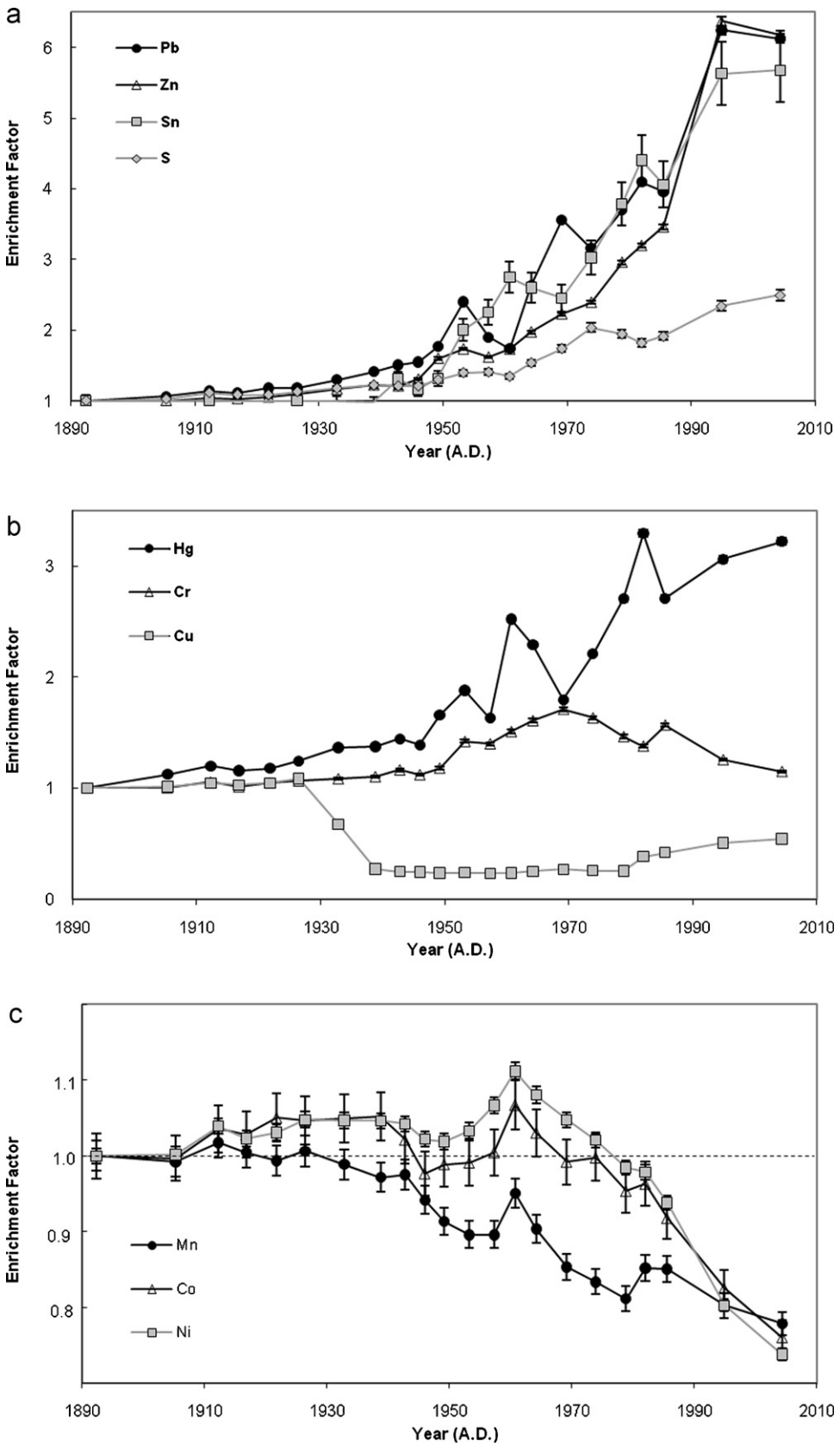

Fig. 7. Temporal record of the Pb, Zn, Sn, S, Hg, Cr, Cu, Mn, Co and Ni enrichment factors. The uncertainties were: Pb (<1%); Zn (<1%); Sn (<8%); S (<3%); Hg (<1%); Cr (<1%); Cu (<1%); Mn (<2%); Co (<5%); Ni (<1%). The slump event (1982) is not included.

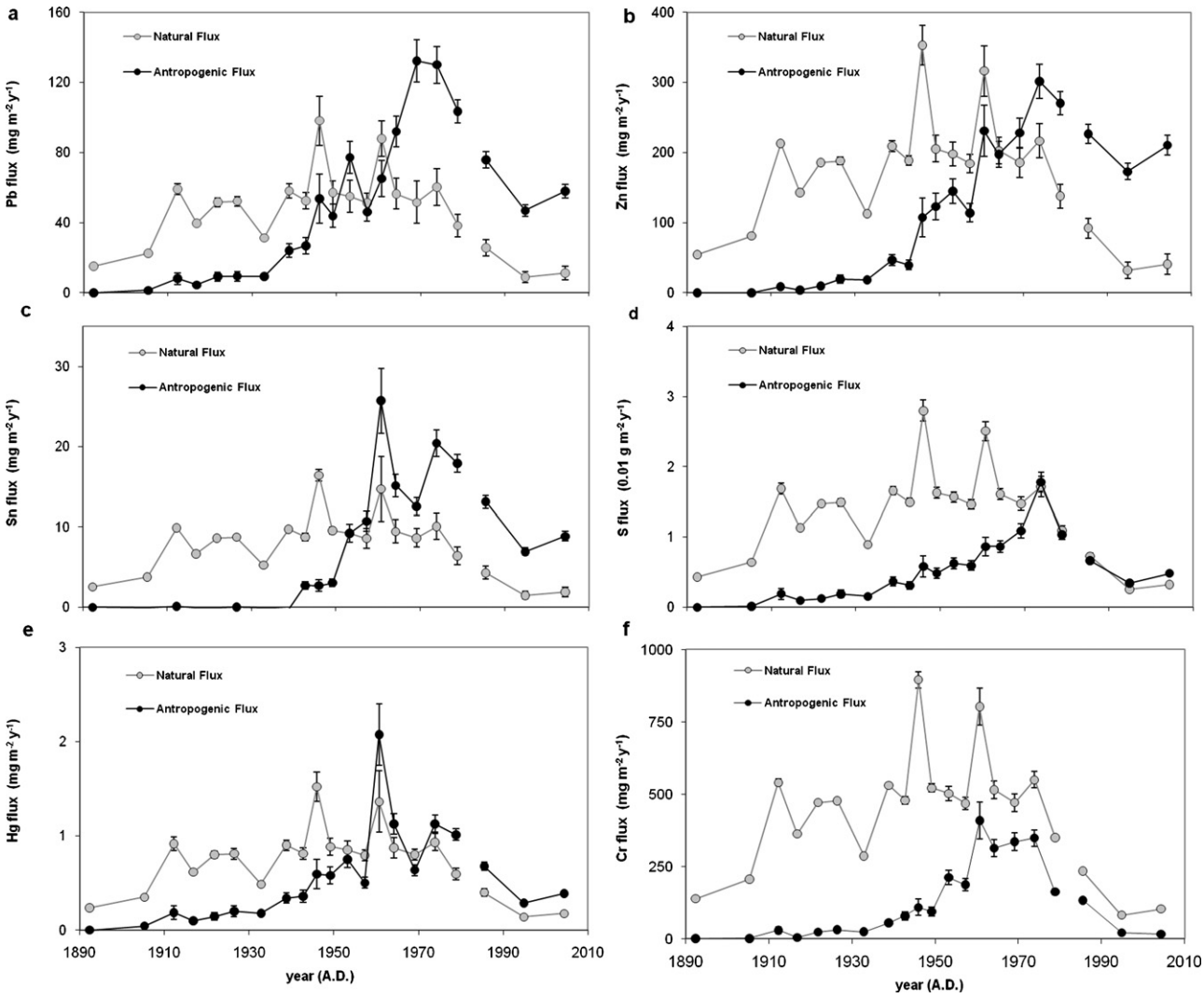

Fig. 8. Reconstructed natural and anthropogenic fluxes of Pb, Zn, Sn, S, Hg and Cr in the last century. The flux due to the slump event (1982) is not included.

are drastically reduced since the 1990s, due to a combination of the coastal zone management program of the Bay and the economic contraction of Cuba.

The EFs of Mn, Co and Ni are close to or below 1 (Fig. 7c), indicating that these elements are depleted towards the surface. The slight decrease of the Mn enrichment factor values towards the core surface (Fig. 7c) could be related to Mn remobilization owed to diagenesis, since it is known that Mn^{3+} reduction to Mn^{2+} in anoxic sediments might promote the dissolution of Mn compounds and the upward diffusion of soluble species into the water–sediment interface [46,47]. This same process could also explain the EF profiles obtained for Ni and Co, which showed a slight deficit at sediment core surface (Fig. 7c.) and whose diagenetic behavior in coastal sediments have been reported to be strongly associated with that of Mn oxides [48]. However, no other trace element profile showed to be influenced by the Mn behavior in the sedimentary column, and Mn, Fe as well as Ni and Co showed significant correlations to Al, indicating that diagenesis influence is not significant on the trace elements depth profiles and that changes observed are mostly due to variations in the trace elements terrestrial input to Havana Bay.

5.3. Change in sediment sources

The PCA analysis showed that two factors explained more than 76% of the total variance (Table 1). Factor 1 explained 41% of the total variance and grouped the typical pollutants (e.g. Pb, Zn, Hg, S, Sn, etc.) with negative values and other elements, like Mn, with

Table 1
Principal component (PC) loadings of PCA based on 25 variables of the core from station B. The largest coefficients in each PC are in bold.

	MAR	Ca	Si	Al	Fe	S	Mn	Pb	Cr	Zn	Cu	As	Co
Factor 1	−0.34	0.62	0.13	0.24	−0.15	−0.97	0.94	−0.97	−0.49	−0.97	0.55	−0.09	0.64
Factor 2	0.69	−0.73	0.96	0.94	0.94	0.16	0.25	0.09	0.69	−0.12	−0.38	−0.52	0.73

	Hg	Ni	Sn	Mg	K	Ti	Br	I	Sr	Ba	Mo	U
Factor 1	−0.84	0.57	−0.93	−0.85	−0,34	−0.01	−0.71	−0.63	−0.36	−0.20	−0.92	−0.66
Factor 2	0.44	0.78	0.23	0.35	0.76	0.93	−0.63	−0.72	0.06	0.32	−0.28	−0.08

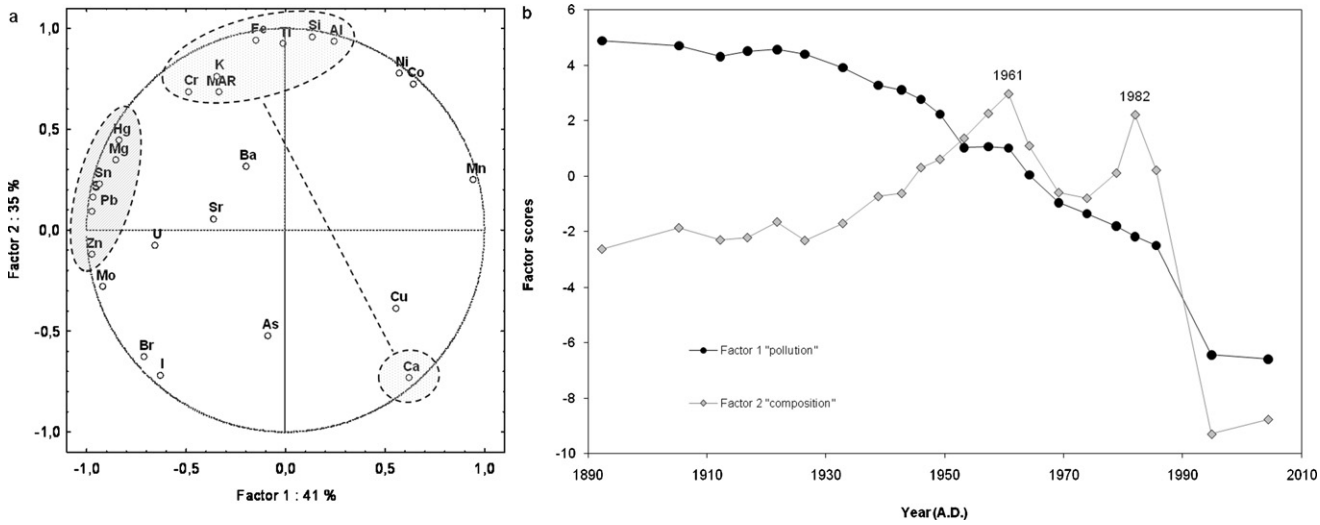

Fig. 9. (a) Projection of 25 variables on the two principal components plane. (b) Temporal evolution of the two principal components.

positive values (Fig. 9a). Factor 2, which explained 35% of the total variance, included the major components of the sediments, and allowed to identify the two main sediment sources: Ca from marine sediments with negative value; Si, Al, Ti and Fe from terrigenous inputs, with positive value (Fig. 9a).

The section loadings for the two main factors showed significant time trends (Fig. 9b). From 1890 to approximately 1930, the sediments showed a constant value of major components (Factor 2) and rather constant pollution levels (Factor 1). From 1930 to 1961, pollution levels steadily increased (decrease of Factor 1), caused by the socio-economic development of the Havana City [2,16], and terrigenous inputs increased due to catchment erosion. In 1957–61 and 1982 we observed a peak of terrigenous components, coincident with high MAR and due to extreme rainfall in Havana. From 1961 to approximately 1990, the pollution levels steadily increased. However, after 1990 the terrigenous input steady decreased while pollution levels steadily increased. These opposite trends reflect the reduction of terrigenous input to the bay due to the socioeconomic contraction from 1993 to 1998 and the coastal zone management actions taken in the Bay and its watershed after 1998. The reduction of the sediment load in the bay had the negative effect of increasing the pollutant concentrations in suspended matter, reflected as enhanced sediment concentration levels, but the positive effect of reducing the total flux of pollutants to the sediment.

6. Conclusions

A sediment core from Havana Bay allowed us to reconstruct the history of anthropogenic impacts since the beginning of the XX century. We observed a steady increase of pollutants (e.g. Pb, Zn, Sn, and Hg) since the beginning of the last century to the mid 90s, with enrichment factors as high as 6. Relative fast decreases of MAR and pollutants were observed after mid 90s, although some concentrations remain high. We concluded that the economic contraction of Cuba and the integrated coastal zone management program introduced in the 90s are responsible for the reduction of sedimentation and pollution fluxes in the Bay. This observation confirmed the positive results of the management program to reduce the suspended matter supply to the bay. However, it is still necessary to implement new actions oriented to reduce the concentration levels of organic matter and metals associated to particulate matter entering the system by further acting on the pollution sources themselves. This work shows the relevance of dated environmental archives to reconstruct the sedimentation and pollution trends and its usefulness to evaluate the impact of environmental management practices.

Peaks of the mass accumulation rates were found to be associated with the time of occurrence of a strong hurricane or a period of intensive rains. Moreover, over the past 60 years, most of the peaks of the MAR occurred in years (1957, 1972 and 1982) characterized by strong El Niño events. This study shows the impact of the ENSO oscillation in coastal estuaries like the Havana Bay.

This historical reconstruction of the environmental changes in Havana Bay provided an excellent example of the use of Nuclear Techniques as tools in the Management Problems of Coastal Zones in the Caribbean Region.

Acknowledgements

This work was supported by the IAEA (Regional Project RLA/7/012) and the CIEMAT International Cooperation program. We also acknowledge the Swiss Federal Office for Public Health (OFSP) for their financial support. This work has involved a large number of people, and it is impossible to list all of them here. We would like to give special thanks to CEAC staff (Anabel Pulido, Hector Cartas, Rosario Rodríguez, Miguel Gómez), CIEMAT staff (Lourdes Romero – in memoriam, Manuel Barrera, Dolores M. Sánchez, Manuel Fernández, Ramón Morante, M. Isabel Rucandio, Rodolfo Fernández), CIMAB staff (Reinaldo Fernández, Jesus Beltran) and IRA staff. We are also grateful to IAEA Technical Cooperation Department (Latin America Section, very specially the RLA/7/012 Project Manager, Jane Gerardo-Abaya), CIEMAT Office of International Cooperation (Félix Barrio) and CIEMAT Director General Juan Antonio Rubio (in memoriam).

Appendix A. Supplementary data

Supplementary data associated with this article can be found, in the online version, at doi:10.1016/j.jhazmat.2011.09.037.

References

[1] ITT, Informe Final Proyecto CUB/80/001, Investigación y Control de la Contaminación Marina en la Bahía de la Habana, PNUMA, UNESCO (1985) (in Spanish).
[2] A. Valdes-Mujica, La Bahia y la ciudad, Pasado, presente y futuro de un ecosistema, El pelicano (2008) 4–11.
[3] T.M. Church, C.K. Sommerfield, D.J. Velinsky, D. Point, C. Benoit, D. Amouroux, D. Plaa, O.F.X. Donard, Marsh sediments as records of sedimentation, eutrophication and metal pollution in the urban Delaware Estuary, Mar. Chem. 102 (2006) 72–95.

[4] M. Díaz-Asencio, C.M. Alonso-Hernández, Y. Bolanos-Álvarez, M. Gómez-Batista, V. Pinto, R. Morabito, J.I. Hernández-Albernas, M. Eriksson, J.A. Sanchez-Cabeza, One century sedimentary record of Hg and Pb pollution in the Sagua estuary (Cuba) derived from ^{210}Pb and ^{137}Cs chronology, Mar. Pollut. Bull. 59 (2009) 108–115.
[5] M.J. Irabien, A. Cearreta, E. Leorri, J. Gómez, J. Viguri, A 130 year record of pollution in the Suances estuary (southern Bay of Biscay), Implications for environmental management, Mar. Pollut. Bull. 56 (2008) 1719–1727.
[6] A.C. Ruiz-Fernández, M. Frignani, C. Hillaire-Marcel, B. Ghaleb, M.D. Arvizu, J.R. Raygoza-Viera, F. Páez-Osuna, Trace metals (Cd, Cu, Hg, and Pb) accumulation recorded in the intertidal mudflat sediments of three coastal lagoons in the Gulf of California, Mexico, Estuaries Coasts 32 (2009) 551–564.
[7] P.H. Santschi, L. Guo, S. Asbill, M. Allison, A. Britt Kepple, L. Wen, Accumulation rates and sources of sediments and organic carbon on the Palos Verdes shelf based on radioisotopic tracers ^{137}Cs, ^{239,240}Pu, ^{210}Pb, ^{234}Th, ^{238}U and ^{14}C, Mar. Chem. 73 (2001) 125–152.
[8] P.G. Appleby, F. Olfield, The calculation of lead-210 dates assuming a constant rate of supply of unsupported ^{210}Pb to the sediment, Catena 5 (1978) 1–8.
[9] J.A. Sanchez-Cabeza, A.C. Ruiz-Fernandez, ^{210}Pb sediment radiochronology: an integrated formulation and classification of dating models, Geochim. Cosmochim. Acta (submitted for publication).
[10] P.G. Appleby, Chronostratigraphic techniques in recent sediments, in: W.M. Last, J.P. Smol (Eds.), Tracking environmental change using lake sediments, vol. 1, Basin Analysis, Coring and Chronological Techniques, Kluwer Academic Publishers, The Netherlands, 2001, p. 576.
[11] J.N. Smith, Why should we believe ^{210}Pb sediment geochronologies? J. Environ. Radioact. 55 (2001) 121–123.
[12] UNSCEAR, Sources and effects of ionising radiation, Report to the General Assembly, vol. 1, Annex C, United Nations Scientific Committee on the Effects of Atomic Radiation, New York, 2000.
[13] P.G. Appleby, N. Richardson, P.J. Nolan, ^{241}Am dating of lake sediments, Hydrobiology 214 (1991) 35–42.
[14] T. Jaakkola, K. Tolonen, P. Huttunen, S. Leskinen, The use of fallout ^{137}Cs and ^{239,240}Pu for dating of lake sediments, Hydrobiology 103 (1983) 15–19.
[15] F. Wu, J. Zheng, H. Liao, M. Yamada, Vertical distributions of plutonium and ^{137}Cs in lacustrine sediments in Northwestern China: quantifying sediment accumulation rates and source identifications, Environ. Sci. Technol. 44 (8) (2010) 2911–2917.
[16] A. Colantonio, R.B. Potter, City profile Havana, Cities 23 (2006) 63–78.
[17] M. Armenteros, A. Pérez-Angulo, R. Regadera, J. Beltrán, M. Vincx, W. Decraemer, Effects of chronic and heavy pollution on macro- and meiobenthos of Havana Bay, Cuba, Rev. Invest. Mar. 30 (2009).
[18] R. Maal-Bared, Comparing environmental issues in Cuba before and after the special period, balancing sustainable development and survival, Environ. Int. 32 (2006) 349–358.
[19] M.H. Loring, R.T.T. Rantala, Manual for the geochemical analyses of marine sediments and suspended particulate matter, Earth Sci. Rev. 32 (1992) 235–283.
[20] J.A. Sanchez-Cabeza, P. Masqué, I. Ani-Ragolta, ^{210}Pb and ^{210}Po analysis in sediments and soils by microwave acid digestion, J. Radioanal. Nucl. Chem. 227 (1998) 19–22.
[21] W.W. Flynn, The determination of low levels of polonium-210 in environmental materials, Anal. Chim. Acta 43 (1968) 221–227.
[22] T.F. Hamilton, J.D. Smith, Improved alpha-energy resolution for the determination of polonium isotopes by alpha-spectrometry, Appl. Radiat. Isot. 37 (1986) 628–630.
[23] F. Luisier, J.A. Corcho Alvarado, Ph. Steinmann, M. Krächler, P. Froidevaux, A new method for the determination at ultra-low levels of plutonium and americium, using high pressure microwave digestion and alpha-spectrometry or ICP-SMS, J. Radioanal. Nucl. Chem. 281 (3) (2009) 425–432.
[24] S. Bajo, J. Eikenberg, Electrodeposition of actinides for alpha-spectrometry, J. Radioanal. Nucl. Chem. 242 (3) (1999) 745–751.
[25] L.G. Bellucci, S. Giuliani, C. Mugnai, M. Frignani, D. Paolucci, S. Albertazzi, A.C. Ruiz Fernandez, Anthropogenic metal delivery in sediments of Porto Marghera and Venice Lagoon (Italy), Soil Sed. Contam. 19 (2010) 1–16.
[26] D.E. Buckley, J.N. Smith, G.V. Winters, Accumulation of contaminated metals in marine sediments of Halifax Harbour, Nova Scotia: environmental factors and historical trends, Appl. Geochem. 10 (1995) 175–195.
[27] A. Palanques, J.A. Sanchez-Cabeza, P. Masqué, L. León, Historical record of heavy metals in a highly contaminated mediterranean deposit: the Besos prodelta, Mar. Chem. 61 (1998) 209–217.
[28] A. Gelen, O. Díaz, M.J. Simón, E. Herrera, J. Soto, J. Gómez, C. Ródenas, J. Beltrán, M. Ramírez, ^{210}Pb dating of sediments from Havana Bay, J. Radioanal. Nucl. Chem. 256 (3) (2003) 561–564.
[29] C. Alonso-Hernandez, M. Díaz-Asencio, A. Munos-Caravaca, R. Delfanti, C. Papucci, O. Ferretti, T.P. Crowe, Recent changes in sedimentation regime in Cienfuegos Bay, Cuba, as inferred from ^{210}Pb and ^{137}Cs vertical profiles, Cont. Shelf Res. 26 (2006) 153–167.
[30] M. Ravichandran, M. Baskaran, P.H. Santschi, T.S. Bianchi, History of trace metal pollution in Sabine-Neches Estuary, Beaumont, Texas, Environ. Sci. Technol. 29 (1995) 1495–1503.
[31] M. Ravichandran, M. Baskaran, P.H. Santschi, T.S. Bianchi, Geochronology of sediments in the Sabine-Neches Estuary, Texas, U.S.A., Chem. Geol. 125 (1995) 291–306.
[32] P.H. Santschi, Y.H. Li, J. Bell, B. Trier, K. Kowtaluk, Pu in the coastal marine environment, Earth Planet. Sci. Lett. 51 (1980) 248–265.
[33] P.H. Santschi, M. Allison, S. Asbill, A.B. Perlet, S. Cappellino, C. Dobbs, L. McShea, Sediment transport and Hg recovery in Lavaca Bay, as evaluated from radionuclide and Hg distributions, Environ. Sci. Technol. 33 (1999) 378–391.
[34] C. Gascó, M.P. Antón, M. Pozuelo, J. Meral, A.M. Gonzalez, C. Papucci, R. Delfanti, Distributions of Pu, Am and Cs in margin sediments from the western Mediterranean (Spanish coast), J. Environ. Radioact. 59 (2002) 75–89.
[35] J.A. Robbins, Geochemical, Geophysical applications of radioactive lead isotopes, in: J.P. Nriago (Ed.), Biochemistry of Lead in the Environment, Amsterdam, Elsevier, 1978.
[36] A. Diaz Arenas, Tropical storms in Central America and the Caribbean. Characteristic rainfall and forecasting of flash floods Hydrology of Humid Tropical Regions with Particular Reference to the Hydrological Effects of Agriculture and Forestry Practice, vol. 140, IAHS Publ., 1983, pp. 39–51.
[37] Opus Habana, El camino del viento, Huracanes sobre La Habana, Opus Habana 3 (2005) 4–13.
[38] C. Oria, Huracanes habaneros y sus insólitas secuelas, TRIBUNA de La Habana (2008).
[39] L. Naranjo Diaz, La Niña Impacts in Cuba: the opposite face of the coin? in: International Workshop La Niña summit: Review of the Causes and Consequences of Cold Events, United Nations University, NCAR, UNEP, Colorado, USA, 1998.
[40] P. Cardenas, M. Perez, Eventos ENOS y anomalias de, las lluvias en Cuba, Technical Report, Instituto de Meteorologia, Havana, Cuba, 1991.
[41] B. Hernandez, El Niño-Oscilación del Sur (ENOS) y los frentes fríos que arriban a la región occidental cubana Invest. Mar. 30 (2) (2002) 3–19.
[42] J. Rubiera, A. Caymares, Severe weather events induced by enso events during the Cuban winter season, Bulletin de l'Institut francais d'études Andins, 27 (3) (1998) 845–855.
[43] A. Chen, A. Roy, J. McTavish, M. Taylor, L. Marx, Using SST anomalies to predict flood and drought conditions for the Caribbean Center for Ocean–Land–Atmosphere Studies Rep., vol. 49, 1997.
[44] J.M. Spence, M.A. Taylor, A.A. Chen, The effect of concurrent sea-surface temperature Anomalies in the tropical pacific and atlantic on Caribbean rainfall, Int. J. Climatol. 24 (2004) 1531–1541.
[45] J. Beltrán, M. Pérez, L. López, R. Regadera, Control y evolución de la calidad ambiental de la Bahía de La Habana, Final Report, Vigilancia ambiental para la, Bahía de La Habana, CIMAB, 2008.
[46] W.S. Reeburgh, Rates of biogeochemical processes in anoxic sediments, Ann. Rev. Earth Planet. Sci. 11 (1983) 269–298.
[47] B.M. Tebo, K.H. Nealson, S. Emerson, L. Jacobs, Microbial mediation of Mn(II) et Co(II) precipitation at the O_2/H_2S interfaces in two anoxic fjords, Limnol. Ocean. 29 (1984) 1247–1258.
[48] S. Audry, G. Blanc, J. Schafer, G. Chaillou, S. Robert, Early diagenesis of trace metals (Cd, Cu, Co, Ni, U, Mo, and V) in the freshwater reaches of a macrotidal estuary, Geochim. Cosmochim. Acta 70 (2006) 2264–2282.